

Non-local ductile damage implementation using three field low order tetrahedral element

H.R. Javani^{1,2}, R.H.J. Peerlings², M.G.D. Geers²

¹*Materials innovation institute (M2i), Delft, The Netherlands;*

²*Eindhoven University of Technology, Eindhoven, The Netherlands;*

1 Introduction

Ductile damage plays a significant role in many forming processes which induce large strains. Coupled damage-plasticity models have become quite successful at predicting the underlying porosity initiation, porosity growth/coalescence and localized deformation. In the present paper we adopt a scalar damage variable which isotropically affects the elastic and plastic response of the material. The model is fully nonlocal to avoid pathological localisation effect. Here we focus on its implementation in a three-dimensional tetrahedral element.

Tetrahedral elements are often used because mesh generators can reliably mesh complex geometries with them. To reduce computational times, low order elements are preferred, but it is well known that when extra constraints are applied these elements may show a poor performance. For instance when dealing with incompressibility or near incompressibility they may show locking behavior. Some approaches have been developed in the literature to avoid this problem. The available approaches can be categorized as follows. (1) Stabilizing mixed elements by enriching the displacement using a bubble function. (2) Using mesh-dependent perturbation terms. (3) Mixed-enhanced strain stabilization. (4) Orthogonal sub-grid scale methods. (5) Finite increment calculus methods. (6) Average nodal pressures or nodal deformation gradients. Here we use a mixed formulation with an additional bubble displacement, because it can be used in large deformations and it can be implemented in a relatively straightforward fashion. For efficiency reasons the displacement bubble is condensed out of the equations at the element level.

In section 2 the mixed version of the coupled damage-elastoplasticity formulation on which the element is based is explained. The Finite element implementation of the model using bubble enriched displacement field is introduced introduced in section 3. A numerical example is given in section 4 to demonstrate the performance of the method and the conclusion is given in section 5.

2 Coupled damage-elastoplasticity model (mixed version)

This section summarises the equations used in the three field model and its implementation. The elastic response of the material is discussed in section 2.1. Section 2.2 explains the plastic evolution. Then the damage growth and non-locality are explained in section 2.3.

2.1 Elastic response

The coupled damage-elastoplasticity model follows exactly the same lines as in [1]. Continuum Damage Mechanics is used, in which the damage variable ω_p represents the effect of damage on the material's mechanical response. The concept of an effective stress is used in order to characterize the effect of the damage [2]. According to this principle the response of a damaged material is given by the constitutive laws of the virgin material in which the (Kirchhoff) stress is replaced by the effective stress [3]

$$\hat{\boldsymbol{\tau}} = \frac{\boldsymbol{\tau}}{(1 - \omega_p)} \quad (1)$$

The establishment of a coupled elasto-plastic damage material model considering finite deformations is based on the multiplicative split of the deformation gradient $\mathbf{F} = \mathbf{F}_e \cdot \mathbf{F}_p$ into an elastic part \mathbf{F}_e and a plastic part \mathbf{F}_p . This multiplicative decomposition inherits all features of the classical models of infinitesimal plasticity [4]. The effective Kirchhoff stress tensor is decomposed as

$$\hat{\boldsymbol{\tau}} = \hat{\boldsymbol{\tau}}^h \mathbf{I} + \hat{\boldsymbol{\tau}}^d \quad (2)$$

in which $\hat{\boldsymbol{\tau}}^h$ is the hydrostatic part of stress and $\hat{\boldsymbol{\tau}}^d$ is deviatoric part. Each of these parts satisfies the following elastic relations:

$$\hat{\boldsymbol{\tau}}^d = G(4\mathbf{I}^s - \frac{1}{3}\mathbf{I} \otimes \mathbf{I}) : \ln \mathbf{b}_e \quad (3)$$

$$\hat{\boldsymbol{\tau}}^h = \frac{1}{2}K\mathbf{I} : \ln \mathbf{b}_e \quad (4)$$

where $\mathbf{b}_e = \mathbf{F}_e \cdot \mathbf{F}_e^T$ is the elastic left Cauchy-Green deformation tensor, which is used as a non-linear measure of elastic strain, and K and G are bulk and shear modulus respectively.

2.2 Plastic deformation

Classical J2 plasticity is used here. This implies that the elastic domain is defined in terms of the effective stress as

$$\hat{\phi}(\hat{\boldsymbol{\tau}}, \hat{\tau}_y) = \hat{\tau}_{eq} - \hat{\tau}_y \leq 0 \quad (5)$$

In equation (5) $\hat{\tau}_{eq}$ is effective stress, which is defined as

$$\hat{\tau}_{eq} = \sqrt{\frac{3}{2} \hat{\boldsymbol{\tau}}^d : \hat{\boldsymbol{\tau}}^d} \quad (6)$$

The evolution of the plasticity related internal variables is obtained by the assumption of associative plasticity [2]:

$$\mathbf{b}_e^\nabla = -2\dot{\gamma} \frac{\partial \hat{\phi}(\hat{\boldsymbol{\tau}}, \hat{\tau}_y)}{\partial \hat{\boldsymbol{\tau}}} \cdot \hat{\mathbf{b}}_e \quad (7)$$

$$\dot{\varepsilon}_p = \dot{\gamma} \frac{\partial \hat{\phi}(\hat{\boldsymbol{\tau}}, \hat{\tau}_y)}{\partial \hat{\tau}_y} \quad (8)$$

$$\dot{\gamma} \geq 0, \quad \hat{\phi}(\hat{\boldsymbol{\tau}}, \hat{\tau}_y) \leq 0, \quad \dot{\gamma} \hat{\phi}(\hat{\boldsymbol{\tau}}, \hat{\tau}_y) = 0 \quad (9)$$

\mathbf{b}_e^∇ in the first of these equations is the Lie derivative of \mathbf{b}_e . Finally plastic hardening is governed by the hardening law

$$\dot{\hat{\tau}}_y = h_\varepsilon \dot{\varepsilon}_p \quad (10)$$

2.3 Damage growth

Combining equations (1) and (3) shows that the damage variable affects the elastic response of the material. Similarly, it also affects the yield surface via (1), (5) and (6). In a nonlocal formulation the evolution of the damage variable, ω_p , in a certain material point not only depends on the loading history of that point, but also on surrounding material points. The damage evolution is governed by the rate law:

$$\dot{\omega}_p = h_\omega \dot{\kappa} \quad (11)$$

where h_ω is a step function

$$h_\omega = \begin{cases} \frac{1}{\kappa_c - \kappa_i} & \text{if } \kappa_i \leq \kappa \leq \kappa_c \\ 0 & \text{otherwise} \end{cases} \quad (12)$$

and κ is a history variable. Damage grows only when κ reaches an initial value κ_i and at $\kappa = \kappa_c$ the material carries no load and fails completely. The evolution of κ is obtained by Kuhn-Tucker relations

$$\dot{\kappa} \geq 0, \quad \bar{\kappa} - \kappa \leq 0, \quad \dot{\kappa}(\bar{\kappa} - \kappa) = 0 \quad (13)$$

in which initially κ is assumed to be κ_i .

In the above equation \bar{z} is a nonlocal damage driving variable which is calculated by averaging a local variable z . The implicit gradient formulation of that averaging reads

$$\bar{z} - \ell^2 \nabla^2 \bar{z} = z \quad (14)$$

where ∇^2 and ℓ are the Laplacian in the current configuration and an internal length parameter respectively. To solve the above Helmholtz PDE there is a need for a boundary condition, which is here of the Neumann type

$$\vec{\nabla} \bar{z} \cdot \vec{n} = 0 \quad (15)$$

with \vec{n} the outward normal. This additional boundary value problem must be solved simultaneously with the equilibrium equation.

The local variable z in it can be chosen in a manner to account for the influence of the stress triaxiality on the damage growth. Here it is taken to be

$$\dot{z} = h_z \dot{\varepsilon}_p \quad (16)$$

In which h_z is of the form proposed by Goijaerts et al. [5]

$$h_z = \left[1 + A \frac{\tau_h}{\tau_{eq}} \right] \varepsilon_p^B \quad \text{with} \quad [x] = \begin{cases} x, & x > 0 \\ 0, & x \leq 0 \end{cases} \quad (17)$$

The influence of the effective plastic strain and triaxiality can be adjusted by selection of the material constants A and B .

3 FEM implementation using enriched mixed formulation

The material behavior described in section 2 is now implemented using a tetrahedral element. To avoid locking we use an independent pressure discretisation together with a bubble displacement enrichment. The implementation of the described model is similar to that of [1], but here, because the mixed form is used, an additional partial differential equation for the effective hydrostatic kirchhoff stress, $\hat{\tau}^h$, has to be satisfied. The derivation of the weak form of the equations is explained in section 3.1 and the discretization of this weak form with attention to the addition of the bubble displacement field is discussed in section 3.2.

3.1 Weak form of the equations

The governing PDEs to be solved simultaneously read:

$$\vec{\nabla} \cdot [(\tau^h \mathbf{I} + \boldsymbol{\tau}^d) \frac{1}{J}] = \vec{0} \quad (18)$$

$$\hat{\tau}^h = \frac{1}{2} K \mathbf{I} : \ln \mathbf{b}_e \quad (19)$$

$$\bar{z} - \ell^2 \nabla^2 \bar{z} = z \quad (20)$$

The related boundary conditions of the above equations read:

$$\vec{u} = \vec{u}^* \quad \text{on } S_u \quad (21)$$

$$\vec{t} = \vec{n} \cdot \frac{\boldsymbol{\tau}}{J} = \vec{t}^* \quad \text{on } S_t \quad (22)$$

$$\vec{\nabla} \bar{z} \cdot \vec{n} = 0 \quad \text{on } S = S_u \cup S_t \quad (23)$$

The weak forms of the PDEs follow by the usual arguments as:

$$\int_{\Omega} (\vec{\nabla} \vec{\phi})^T : (\tau^h \mathbf{I} + \boldsymbol{\tau}^d) \frac{1}{J} d\Omega = \int_{\Gamma} \vec{\phi} \cdot \vec{q} d\Gamma \quad (24)$$

$$\int_{\Omega} \psi (\hat{\tau}^h - \frac{1}{2} K \mathbf{I} : \ln \mathbf{b}_e) d\Omega = 0 \quad (25)$$

$$\int_{\Omega} (\phi_{\bar{z}} \bar{z} + \ell^2 \vec{\nabla} \phi_{\bar{z}} \cdot \vec{\nabla} \bar{z} - \phi_{\bar{z}} z) d\Omega = 0 \quad (26)$$

where $\vec{\phi}$, ψ and $\phi_{\bar{z}}$ are weight functions corresponding to \vec{u} , $\hat{\tau}^h$ and \bar{z} .

3.2 Discretization using bubble enrichment of the displacement

Standard discretization of the weak forms derived in section 3.1 results in a system of equations which shows an overly stiff response, which is commonly termed locking. The treatment that we use here is that the displacement and the corresponding weight function are split into contributions in two spaces

$$\vec{u} = \vec{u}' + \vec{u}'' \quad (27)$$

$$\vec{\phi} = \vec{\phi}' + \vec{\phi}'' \quad (28)$$

The term \vec{u}' (and $\vec{\phi}'$) is discretised using the standard linear shape functions. The additional displacement field \vec{u}'' vanishes on the element boundaries and therefore has no effect on the overall displacement. Although it will be condensed out of the equations at the element level, it will greatly improve the element's performance. The interpolation for the bubble displacement and weighting function is given in terms of the volumetric coordinates $\lambda_1, \lambda_2, \lambda_3$ associated with tetrahedron as

$$N'' = 256\lambda_1\lambda_2\lambda_3(1 - \lambda_1 - \lambda_2 - \lambda_3) \quad (29)$$

The hydrostatic Kirchhoff stress, $\hat{\tau}^h$, non-local damage driving variable, \bar{z} , and standard displacement, u' , and their corresponding weight functions are interpolated linearly within the element - see Figure 1. We denote the discretisation thus introduced

$$\vec{u}' = \underset{\sim}{N}'^T \underset{\sim}{\vec{u}}' \quad (30)$$

$$\bar{z} = \underset{\sim}{N}'^T \underset{\sim}{\bar{z}} \quad (31)$$

$$\hat{\tau}^h = \underset{\sim}{N}'^T \underset{\sim}{\hat{\tau}}^h \quad (32)$$

$$\vec{u}'' = \underset{\sim}{N}''^T \underset{\sim}{\vec{u}}'' \quad (33)$$

Application of the discretisation to the weak form and subsequently eliminating the coefficients of the weight functions results in a system of nonlinear equations of the form

$$\underset{\sim}{\vec{F}}'_{int} = \underset{\sim}{\vec{F}}'_{ext} \quad (34)$$

$$\underset{\sim}{\vec{F}}''_{int} = \underset{\sim}{\vec{0}} \quad (35)$$

$$\underset{\sim}{F}^{\tau^h}_{int} = \underset{\sim}{0} \quad (36)$$

$$\underset{\sim}{F}^{\bar{z}}_{int} = \underset{\sim}{0} \quad (37)$$

in which the following terms have been used

$$\vec{F}'_{\sim ext} = \int_{\Gamma} \vec{N}' \vec{q} d\Gamma \quad (38)$$

$$\vec{F}'_{\sim int} = \int_{\Omega} \vec{\nabla} \vec{N}' \cdot (\tau^h \mathbf{I} + \tau^d) \frac{1}{J} d\Omega \quad (39)$$

$$\vec{F}''_{\sim int} = \int_{\Omega} \vec{\nabla} \vec{N}'' \cdot (\tau^h \mathbf{I} + \tau^d) \frac{1}{J} d\Omega \quad (40)$$

$$F^{\tau^h}_{\sim int} = \int_{\Omega} \vec{N}' (\hat{\tau}^h - \frac{1}{2} K \mathbf{I} : \ln \mathbf{b}_e) d\Omega \quad (41)$$

$$F^{\bar{z}}_{\sim int} = \int_{\Omega} (N' \bar{z} + \ell^2 \vec{\nabla} \vec{N}' \cdot \vec{\nabla} \bar{z} - N' z) d\Omega \quad (42)$$

where \vec{q} is the traction vector, \vec{N}' and \vec{N}'' are the columns of shape functions and $\vec{\nabla}$ is the gradient with respect to the current coordinates. The Backward-Euler method is used to calculate all history dependent variables in (39)-(42).

We linearise and then condense out one equation per element which finally results in three sets of equations to be simultaneously solved instead of four. The solution to the aforementioned system of equations consists of three displacement components, one hydrostatic Kirchhoff stress and one non-local damage driving variable per corner node, as well as three bubble displacements in the node interior to the element as shown in figure 1.

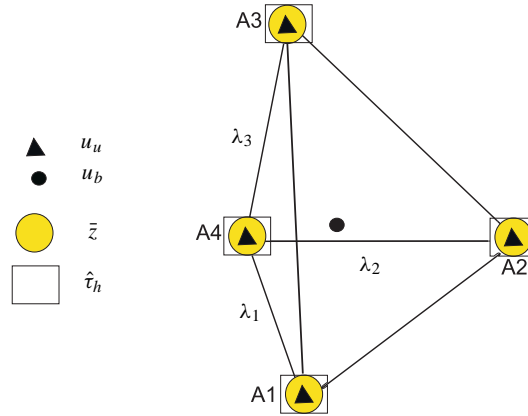


Figure 1: Location of the bubble node in the tetrahedral element.

4 Numerical example

To study the performance of the element a variant of Cook's membrane problem is investigated in a three dimensional simulation. It consists of a tapered plate clamped

Table 1: Material properties used in the Cook's membrane test.

Shear modulus G	80.19 GPa
Bulk modulus K	164.21 GPa
Initial flow stress τ_{y0}	0.45 GPa
Residual flow stress $\tau_{y\infty}$	0.715 GPa
Linear hardening coefficient h	1.290 GPa
Saturation exponent α	16.93
Damage initiation threshold κ_i	0.05
Critical value of history parameter κ_c	0.90
Intrinsic length ℓ	2 mm
Damage parameter A	14
Damage parameter B	0.5

at one of its sides while a shearing displacement acts on the other side - see Figure 2. One element through the thickness is used and all surface nodes in the three dimensional mesh are constrained in the direction perpendicular to the plane of the sketch in order to have a plane strain situation. A vertical displacement of $u = 7$ mm is applied to the nodes on right edge of the plate. In our simulations, we compare the performance of the standard isoparametric formulation (linear tetrahedral) and the formulation developed above. The material parameters are chosen in a way to

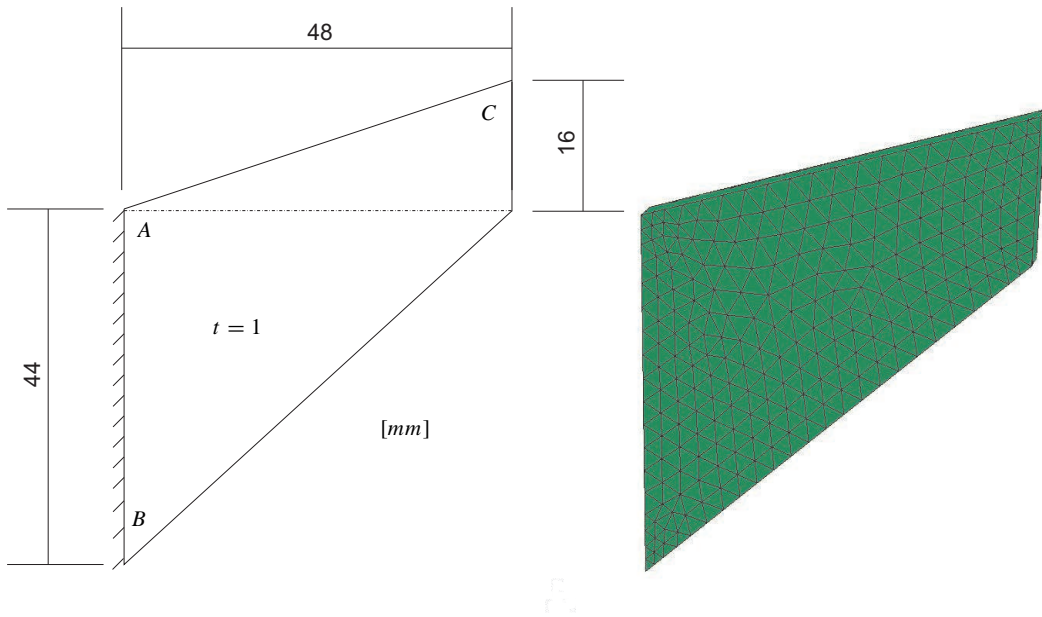


Figure 2: Geometry and finite element discretization of the model.

induce damage during deformation. Table 1 shows the material properties used in this test.

The reaction force on the right edge of the plate versus the displacement as obtained with the methods indicated above is compared to that obtained by the standard element. Figure 3 demonstrates that upon refining the mesh, the curves associated with the standard element are tending to converge to a unique solution.

The figure clearly shows that the coarsest standard isoparametric formulation overestimates the force. The force versus displacement curve obtained using the new element in a coarse mesh is much closer to the refined meshes using the standard formulation and thus does not show a pathologically stiff behaviour. This element thus has the ability to generate more accurate solutions even for coarse discretisations at a limited additional cost. Figure 4 shows the damage distribution at the end of the deformation process.

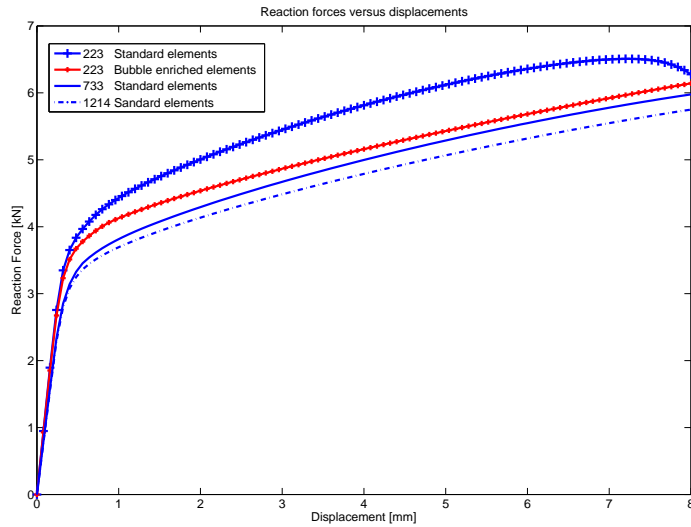


Figure 3: Force versus displacement of the standard and new element while using different mesh refinement.

5 Conclusion

We have presented an implementation of a three-field low-order non-local elastoplastic damage element which prevents locking. In this implementation an additional field, the hydrostatic Kirchhoff stress, is discretised and the element displacement is enriched by a bubble. The enrichment does not add much to the calculation time as it is condensed out at the element level. The element performance is tested by using a benchmark problem and it shows superiority over the standard elements in dealing with incompressibility.

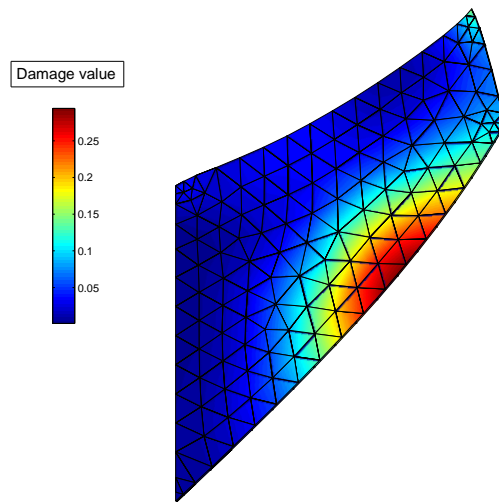


Figure 4: Distribution of damage within the plate.

References

- [1] J. Mediavilla, R.H.J. Peerlings, M.G.D. Geers, 2006. *A nonlocal triaxiality-dependent ductile damage model for finite strain plasticity*, Computer Methods in Applied Mechanics and Engineering, **195**, 4617-4634.
- [2] Lemaitre, J., 1992. *A Course on Damage Mechanics*. Springer.
- [3] P.I. Kattan, G.Z. Voyiadjis, 2001. *Damage mechanics*. Springer.
- [4] Simo, J.C., 1992. *Algorithms for static and dynamic multiplicative plasticity that preserve the classical return mapping schemes of the infinitesimal theory*. Computer Methods in Applied Mechanics and Engineering, **99**, 61-112. Springer.
- [5] Goijaerts, A.M., Govaert, L.E. and Baaijens, F.P.T., 2001. *Evaluation of ductile fracture models for different metals in blanking*. Journal of Materials Processing Technology, **110**, 312-323.